JOURNAL OF MATERIALS SCIENCE **36** (2001) 1007–1013

Cellular arrays of alumina fibres

H. X. PENG, Z. FAN
Department of Materials Engineering, Brunel University, Uxbridge, Middlesex, UB8 3PH, UK

J. R. G. EVANS
Department of Materials, Queen Mary and Westfield College, University of London, Mile End Road, London E1 4NS

In conventional short fibre reinforced metal matrix composites, the quest is for a method of processing that will provide a homogeneous and preferably random arrangement of fibres. In contrast, recently developed contiguity models for multiphase composites on the one hand, and finite element modelling of structures on the other, independently predict that the modulus enhancement provided by short-fibre reinforcement can be improved if the fibres are arranged in a cellular structure. Furthermore, provided the metallic phase is continuous, the toughness of the composite may also thereby be enhanced. This paper, which is part of an attempt to explore the question of reinforcement arrangements, presents a method for making ceramic preforms for MMCs in which a polymeric foam is used to position the fibres in cellular array. The polymer is then removed by pyrolysis and the preform of fibres is strengthened by sintering. During high temperature sintering, phase changes and grain growth degraded the fibre. Methods of increasing the compressive strength of the preform by incorporation of alumina particles and by subsequent infiltration are described and compared.

1. Introduction

Besides the obvious refractory applications for ceramic foams, reticulated ceramics that have open porosity, are used primarily in applications where fluid transport within the microstructure is required [1]. These may include catalyst supports, molten metal filtration or hot gas filtration, but the application which motivates the present work is the use of reticulated structures as preforms for metal matrix composites (MMCs). There is a need to develop processing techniques which will provide the microstructure of a two-phase, three-dimensionally inter-connected composite after melt infiltration [2]. Several reviews of ceramic foams and their fabrication have recently appeared, including those by Saggio-Woyansky, Scott and Minnear [3] Sepulveda [4] and Rice [5]. They provide an effective way to control the distribution of the reinforcement in composite materials and hence to influence the properties such as modulus, conductivity and dielectric constant.

One of the established methods of preparing metal matrix composites is squeeze casting in which molten metal infiltrates a porous preform consisting of ceramic fibres. The emphasis until recently, has been on attempting to produce homogeneous isotropic preforms.

However, a theoretical model based on a microstructural approach allows the physical properties to be predicted [6–8]. One of the outcomes of this model is that the mechanical and physical properties depend more directly on the continuous volume fraction of reinforcement than on the overall volume fraction. The model therefore suggests that, for a fixed volume fraction of the same reinforcement, a composite with two networks: a metallic network and a fibre-reinforced MMC network should present an elastic modulus that is higher than that obtained by a random reinforcement distribution. Since the metal matrix is continuous, it should also offer better damage tolerance. The same conclusion has been obtained by the topological optimisation of structural elements using finite element analysis [9]. This coincidence of conclusions of theoretical models offers sufficient justification to explore the property advantages that are expected to accrue from the use of controlled inhomogeneous structures in MMCs.

The approach to structure control was to employ a polymer processing method capable of preparing ceramic foams [10] and to replace the powder with short staple ceramic fibres.

Generally, the fabrication method selected for making ceramic foams determines the range of porosity, the pore morphology and pore size distribution. Previous work has indicated that conventional and commercially available polyurethane systems can be used to produce ceramic foams [10–12] in which microstructural control of the final foam during the processing step is possible.

A tangled fibre network is one of the four basic structures of porous ceramics [13] and the method for making such fibre networks as preforms normally involves mixing the fibres with water followed by slurry and filter pressing which yields a random or planar random distribution of fibres. Although directional arrangement, such as a planar random distribution [14], has been

achieved by some manufacturers, there is less control in the spatial distribution of the fibres due to the limitations of the process.

The method employed here, based on the procedure used in our previous work for particulate ceramic foams [10, 15], presents a method for arranging short fibres in an efficient way to form cellular structures for the subsequent melt infiltration of metals. It thus uses a polymer processing operation to make a ceramic structure for a metallurgical goal.

2. Experimental details

A two-component, polyurethane (PU) foaming system (grade ISOFOAM RM6216W) was supplied by Baxenden Chemicals (Accrington, Lancs, UK). The details have been described elsewhere [15].

The ceramic fibre selected for this study was Saffil alumina short fibre which is predominantly δ-alumina (Al_2O_3) with an average diameter of 3 μm and a fibre length ranging from 100 to 150 μm. This was kindly donated by Vernaware, Bolton, UK. Table I gives the basic properties of the fibre and its morphology is shown in Fig. 1 at low magnification (a) and, in order to show the smooth surface of the fibre, at higher magnification (b).

The processing sequence is summarised in Fig. 2 and the details are similar to those used for the preparation for particulate ceramic foams [12]. All the suspensions prepared for foaming contained 5 vo1.% fibre mixed into both components of the system. This was the maximum volume fraction of fibre that retained fluidity as found by introducing different amounts of fibre into the components of the foam. Beyond this value, the suspension was too viscous to foam.

In order to enhance mechanical strength of the cellular body, silicone oil (Dow Corning 510/50cS, BDH Laboratory Supplies, Poole, UK) or alumina powder were incorporated in the foaming system during the processing procedure. A siliceous phase produced by the decomposition of silicone oil provides a binder which can be employed in strengthening porous ceramic bodies. Alumina powder (MA130 grade, D_{50} of 4 μm, supplied by Alcan Chemicals Europe, Burnt Island, Scotland) was added to increase the number of particle-fibre bridges. The compositions of these modified foaming systems are given in Table II.

An alternative method of introducing ceramic powder for the purpose of strengthening the cellular body was as follows. The sintered foams with coarse powder additive were infiltrated with the fine alumina powder (RA45E, supplied by Alcan Chemicals Europe, Burnt Island, Scotland) in suspension on up to three occasions. After infiltration, they were dried at 200 °C for at least 12 hrs and then fired at 1200 °C for 2 hr. In order to prepare suspensions for infiltration, sedimentation tests were carried out on 5 vol.% alumina suspensions adjusted to pH 1.7, 8.5 and 12 as measured by a model PW9418 meter (Philips, UK) calibrated with a pH4 buffer. The suspension that showed least sedimentation was selected for infiltration.

TABLE I Properties of Saffil alumina fibre (RF grade)

Chemical composition	Al_2O_3: 96–97% SiO_2: 3–4%
Crystal phase	mainly δ-alumina*
Density	3300 kg/m^3
Median fibre diameter	3 μm
Melting point	>2000 °C
Tensile strength	2000 MPa
Young's modulus	300 GPa

*Alpha alumina <15%, as claimed by the manufacturer.

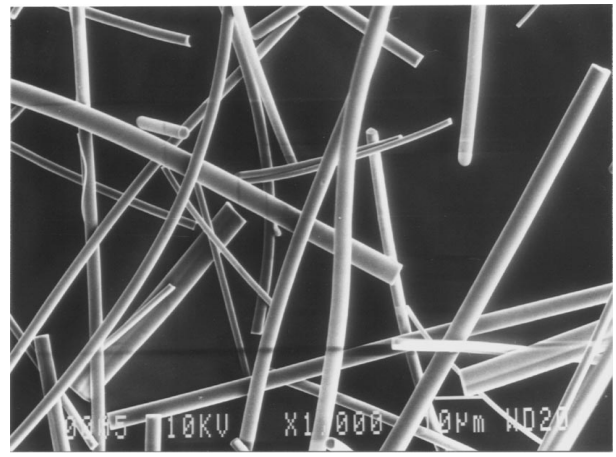

(a)

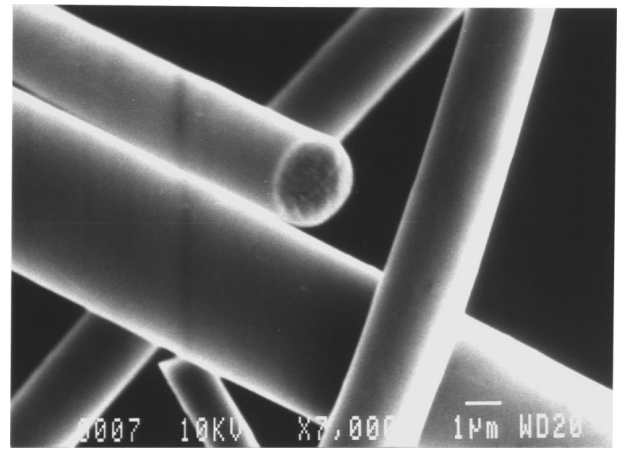

(b)

Figure 1 Morphology of Saffil short alumina fibre (a) low magnification and (b) high magnification showing smooth surface.

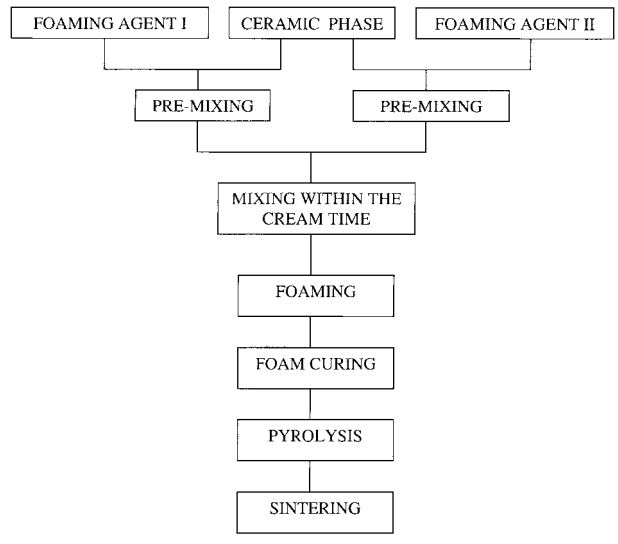

Figure 2 Flow chart of the processing procedure for ceramic foams.

TABLE II Compositions for preparation of fibre foams

Sample	Composition vol.%+			
	Alumina fibre	Powder	Silicone oil	Polyurethane
Fibre foam without additives	5	0	0	Bal.
Fibre foam with powder addition	5	0.5	0	Bal.
Fibre foam with silicone oil	5	0.5	0.25	Bal.

+Based on the ceramic-polymer system.

A phase transformation occurs between different crystalline polymorphs of alumina during heat treatment. The as-received fibres were fired at 1200 °C and 1650 °C for 2 h and the phase composition and fibre morphology were examined by X-ray diffraction (XRD) and scanning electron microscopy (SEM).

Thermogravimetric analysis (TGA) was carried out on the foamed suspension in order to judge the pyrolysis and sintering schedules. A Perkin-Elmer Model TGS-2 analyser was used with a flow rate of air of 25 ml/min and a heating rate of 10°C/min.

The polymer-ceramic foam was cut into cubes of side 40 mm and pyrolysed in flowing air (41/hr) at 5 °C/hr to 450 °C with a 2 hour hold before furnace cooling. Sintering was carried out in air with a heating rate of 2 °C/min to 1200 °C with a 2 hour hold before furnace cooling.

The microstructure of the foams was observed by using a Jeol JX840 scanning electron microscope (SEM) where the samples were secured with double sided conducting tape. No liquid adhesives or dags were used. The compressive strength of the sintered foam was measured using a Model 4206 Instron testing machine (Instron Ltd, Buckinghamshire, UK) fitted with flat steel platens closing with a cross head speed of 0.5 mm/min.

3. Results and discussion

3.1. Thermogravimetry and phase transformation

The thermogravimetric weight loss (Fig. 3) of a pure fibre foam shows a three stage decomposition of the cured polyurethane culminating in the loss of carbonaceous residue at ∼630°C in air. The final residue is

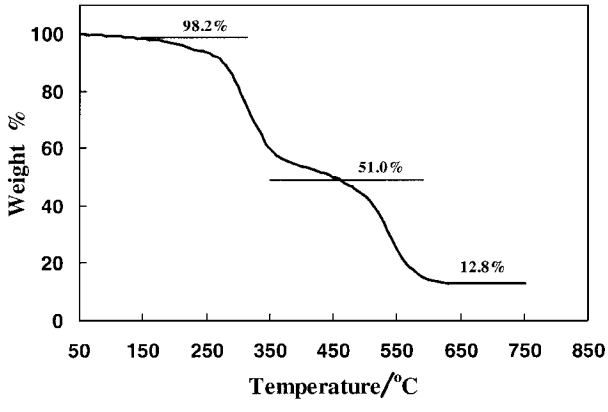

Figure 3 The TGA curve of a pure fibre foam showing a two stage polymer decomposition.

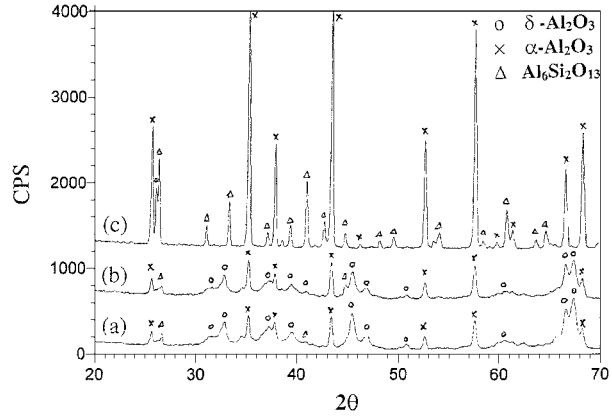

Figure 4 XRD results showing the phase transformation of alumina fibre during high temperature treatment. The as-received fibre is also shown for comparison: (a) as-received (b) sintered at 1200°C for 2 hr (c) sintered at 1650° C for 2 hr.

12.8%wt which is equivalent to the starting weight percent of the fibre phase in the suspension within the experimental error. On this basis, the heating schedule described in Section 2 was devised for samples of 40 mm cube. Because of the low apparent thermal conductivity of these low density foams, larger samples may need much lower heating rates. After pyrolysis, the preform was black due to traces of residual carbon from the polymer phase.

The phase transformation during high temperature treatment revealed by XRD is shown in Fig. 4. The XRD trace of the as-received fibre is also shown for comparison (Fig. 4a). The as-received fibre is composed of mainly δ-alumina and α-alumina but the peaks are not sharp due to the fine grained structure [16]. The peak intensities of the α-alumina increased slightly when the sample was heated at 1200 °C for 2 hours and correspondingly, those of the δ-alumina decreased (Fig. 4b). This indicated that partial phase transformation from δ to α-alumina occurred at 1200 °C in agreement with the findings of Birchall and co-workers [16] and this was accompanied by a morphological change of the fibre surface which is shown below. There are also a few peaks corresponding to $Al_6Si_2O_{13}$ which appeared after heat treatment at 1200 °C, due to the reaction between Al_2O_3 and the 3–4 wt% SiO_2 which exists in Saffil fibre (Table I).

After sintering at 1650 °C for 2 hours, the transformation went to completion and the peaks of α-alumina are very sharp due to extensive increase in grain size (Fig. 4c). The peaks of $Al_6Si_2O_{13}$ are remarkably well defined as well.

The surface morphology changes resulting from the phase transformations and grain growth of the fibre after high temperature treatment are shown in Fig. 5. For samples sintered at 1200 °C, the edges of a plate-like phase appear on the fibre, both on the surface and inside (Fig. 5a) which are believed to reflect the phase transformation and grain growth [16]. The time-temperature conditions determine the conversion rate which, as shown by Badkar and Bailey [17], is controlled by the interaction of the phase boundary with pores.

With the nucleation and growth of the alpha alumina phase, grain boundaries become more obvious at the

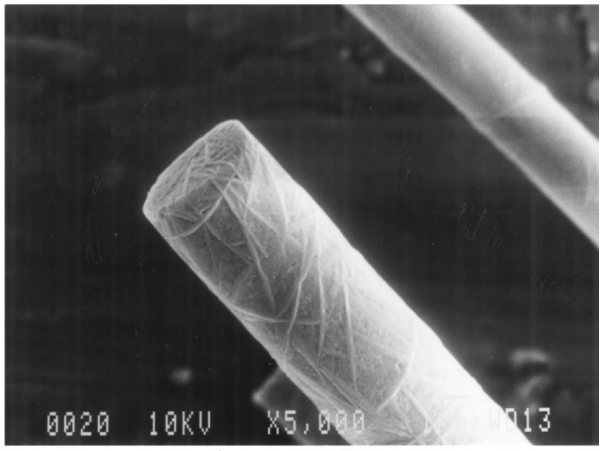

(a)

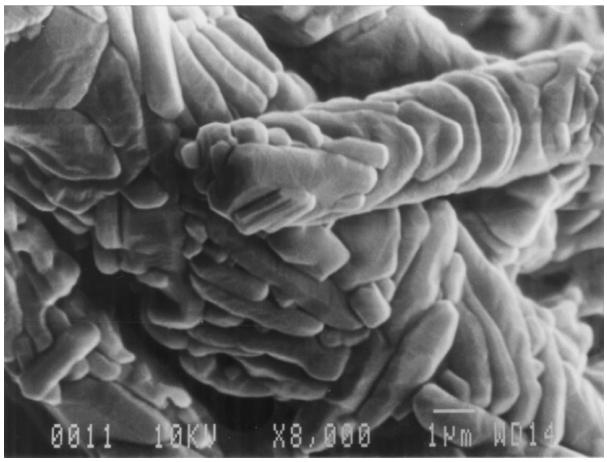

(b)

Figure 5 The surface morphology changes resulting from high temperature treatment (a) sintered at 1200°C for 2 hr (b) sintered at 1650°C for 2 hr.

fibre surface. Sintering at 1650 °C for 2 h caused the surface to be distinctly changed. The grain size of the α-alumina is several microns (Fig. 5b). This is much larger than that of the original grain size (about 50 nm) in the fibre as suggested in Dinwoodie's work [16]. Previous studies [14, 16] indicate that this transformation incurs a loss of fibre properties; the tensile strength decreases dramatically when the fibre is subjected to high temperature heat treatment.

In this study, the sintering of the final fibre foam was carried out at 1200 °C for 2 hrs in order to achieve adequate strength and limit damage to the fibre itself. Since lower temperatures offer little or no sintering, this is a compromise.

Table III gives a summary of the relative densities and volumetric shrinkage at each stage in the process. For each foam, a substantial shrinkage occurs as the polymer is removed and again during sintering and this is a disadvantage when high dimensional accuracy is needed. The shrinkage on pyrolysis establishes the pre-fired relative density at which the fibre assemblies enters the sintering furnace. The volumetric shrinkages for the foams without silicone oil were about 50%, The pre-fired alumina fibre preform underwent a very high shrinkage at the sintering stage, i.e., 90%, and this led to a fired relative density of 4%. This indicates 96% void fraction which is made up of both macroporous and inter-fibre pores.

3.2. Microstructure of the fibre foam

Fig. 6 shows a fracture surface of the foam made without any additives, i.e., fibre only. The cellular structure which is sought for metal matrix composite preforms was successfully achieved by using this foaming method. The fibres have aligned themselves along the longitudinal direction of the struts to form fibre bundles. While this provides a microstructure for the metal matrix composite that should offer high tensile strength in the struts, it also tends to reduce the compressive strength of the preforms because it allows for fewer fibre bridges. Thus, there is less bonding between the fibres in the struts and this tends to result in low strength of the preform. Indeed the foam was too fragile to be handled or tested.

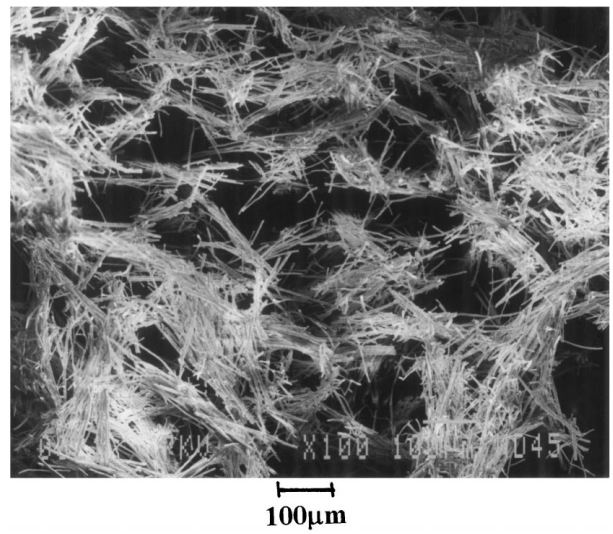

Figure 6 Fracture surface of the foam made without any additives showing the cellular structure but limited bonding between struts.

TABLE III Dimensional changes and volumetric shrinkage during pyrolysis and sintering

Details of sample	As-foamed density (kgm^{-3})	Volumetric shrinkage on pyrolysis	Volumetric shrinkage on sintering	Calculated relative density (%)	Measured relative density (%)
Fibre foam without additives	71	51	86	4.0	4.1
Fiber foam with powder addition	65	44.0	90	4.6	4.2
Fibre foam with silicone oil	344	22.3	32	3.9	4.0

The low strength of the fibre preform results not only from fibre alignment but also from the low volume fraction of fibre that can usefully be incorporated in the liquid components of the resin. This is mainly a result of the high aspect ratio [18, 19]. When higher volume fraction mixtures were prepared, the suspension viscosity rose steeply and very little expansion occurred on foaming. Furthermore, the mechanical strength of junctions between fibres is expected to be low after sintering at 1200°C and mechanical strength of fibres themselves is low after sintering at 1650°C.

In order to increase the number density of contacts, a coarse alumina powder with a mean diameter of 4 μm (MA130) was introduced into the suspensions at an additional volume percent of 10% based on the fibre phase, that is, 0.5 vol.% in the whole suspension. The final structure of the fibre foam produced therefrom is shown in Fig. 7a, and at a higher magnification in Fig. 7b. With the assistance of the alumina powder, the junction density in the fibre struts is increased.

The fibre preform structure shown in Fig. 7 should provide a combination of i) high density of reinforcement in the struts, ii) continuity of the unreinforced ductile metal phase through the open windows of the fibre foam which is regarded as important for toughness of the final MMC and iii) high contact density inside the struts to give high preform strength.

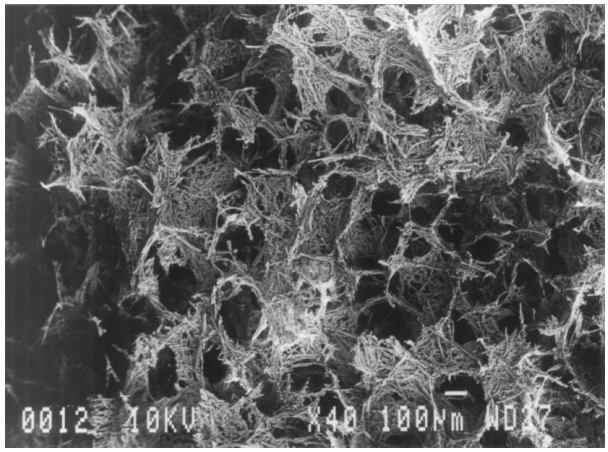

(a)

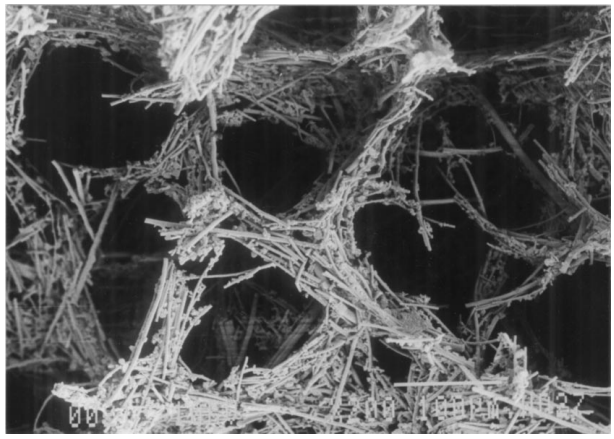

(b)

Figure 7 Microstructure of the fibre foam produced with coarse powder addition and sintered at 1200°C for 2 hrs, (a) low magnification and (b) high magnification.

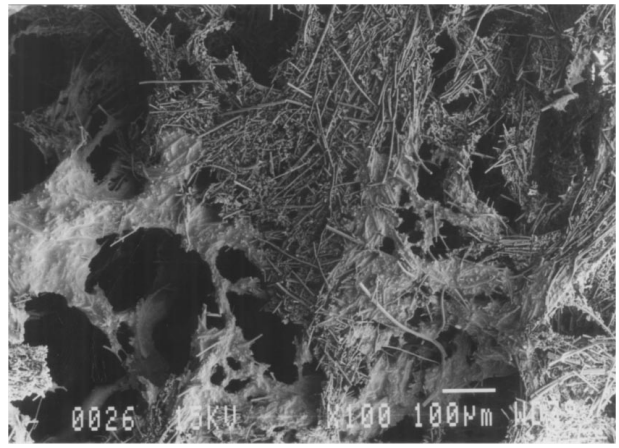

Figure 8 SEM micrograph of the foam produce with silicone oil addition showing non-uniform distribution of residue.

Despite this progress, compressive testing of this foam revealed poor strength. In an attempt to ameliorate the strength, an additive that would leave a siliceous residue was used on the grounds that it would strengthen fibre junctions after a low temperature treatment. Silicone oil which has been added to other ceramic bodies for similar reasons [20] was incorporated in the foaming system. Thermogravimetry of the silicone oil showed that a residue of 4% was left after heating to 800 °C in air. The resulting microstructure of the foam (Fig. 8) was very non-uniform, probably because of the immiscibility of silicone oil in the polymer system. This was later confirmed by observing the phase separation that occurred after thorough mixing of the resin and silicone oil. Also, as shown in Table III, the addition of silicone oil limited the foaming of the suspension and led to a relatively higher as-foamed density and a lower volumetric shrinkage during the pyrolysis and sintering process.

It is arguable that strength could be increased by high temperature sintering because it would strengthening the fibre junctions, but after sintering at 1650°C, the surface morphology of Saffil fibre became grooved due to the phase transformation to α-alumina and grain growth. Previous investigations [14, 16] indicated that high temperature heat treatment (above 1200°C) results in a sacrifice of fibre strength.

3.3. Slurry impregnation of the fibre foam and its effect on compressive strength

The compressive strength of the fibre foam with coarse powder additions was 73 kPa. The target value of compressive strength based on slow infiltration of a non-wetting liquid was estimated as 100 kPa. In order to increase the compressive strength of the ceramic foam to a level that can sustain molten metal influx by squeeze casting, the foam sintered at 1200°C which had been made with addition of coarse alumina powder was subsequently dipped in a fine alumina powder suspension. A fine grade of alumina powder (RA45E) with a mean particle diameter of 0.48 μm was mixed with distilled water at 5 vo1%. In the sedimentation test described in Section 2, the pH of the suspension that gave the longest sedimentation time was pH 11–12. This is more alkaline

than the pH of the isoelectric point for alumina that is generally in the region of 8.5–9 [21].

The sintered foam was dipped in the suspension gradually until the block was completely immersed. This method ensures the outgoing air escaped from the top surface of the sample. After a dwell time of ∼1 minute, the samples were dried at 200 °C for 10 hrs and then sintered at 1200 °C for 2 hrs. For multiple dip experiments, the samples were dried at 200 °C for 10 hrs and sintered at 800 °C after each dip to ensure that the powder would not fall out during handling or subsequent dipping. The weight changes and the total volume fractions of the samples are summarised in Table IV.

Compressive testing was performed on rectangular blocks with a size of 15 × 10 × 10 mm. These results are also given in Table IV. The fibre foam with coarse powder additive before dipping had a compressive strength of 73 kPa. It was too fragile to sustain squeeze casting. After infiltration three times, the strength was increased to 290 kPa. This is strong enough to withstand the pressure encountered in squeeze casting and therefore is suitable for preparing metal matrix composites. Infiltration with the fine powder suspension significantly increased the total volume fraction of the ceramic phase in the foam. The fine powder mainly exists in the struts as shown in Fig. 9. After sintering, the powder sticks to the fibres and leads to an increased number density of contacts and hence to a better bonding between the fibres with consequent increase in the strength of the foam.

TABLE IV Weight changes, total volume fraction of ceramic phase and compressive strength of foams modified by infiltration with 5 vol% RA45E powder suspension

	Before infiltration	Infiltration by one dip	Infiltration by two dips	Infiltration by three dips
Mass (g)	0.49*	0.87	1.22	1.54
Total volume fraction of ceramic (%)	4.20	6.80	9.30	11.50
Compressive strength (kPa)	73	100	157	290

*Initial mass of the sintered foam block before dipping in the powder suspension.

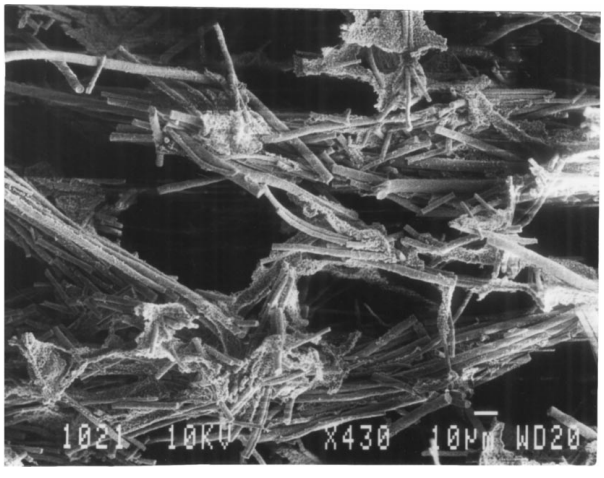

Figure 9 Microstructure of the foam after infiltration with fine powder suspension showing that the fine powder mainly resides in the struts.

The mechanical properties of cellular materials can be related to $C\,(1 - V_p)^m$, where C is a geometric constant characteristic of the unit cell shape, V_p is the volume fraction of the pores and m depends on the deformation mode of the struts [22].

Models for mechanical behaviour often rest on the assumption that the mechanics of a single unit cell can be used to describe the overall deformation. They conclude that the most important factor affecting the mechanical behaviour is the relative density, but they also identify some influence of the cell size on the properties. One expression developed to describe the dependence of compressive strength (σ_{fc}) of open cell ceramics on relative density gives [22]:

$$\sigma_{fc}/\sigma_{fs} = C\,(1 - V_p)^{3/2}. \quad (1)$$

Here, C is a constant that depends on the cellular geometry and has been found empirically to be approximately 0.2 for brittle open-cell foams. For cellular solids with fully dense struts, σ_{fs} is the fracture strength of the dense ceramic material which, for a brittle solid, is close to its fracture stress in simple tension and $(1 - V_p)$ is equal to the relative density.

In the case of fibre arrays described here, infiltration with fine alumina particles did not decrease the pore volume very much and hence the improved strength of the cellular body shown in Table IV is primarily due to the increase in strength of the struts. In the present work, the strut consists of fibres and incorporated particles and is not itself fully dense, so that in Equation 1, $(1 - V_p)$ is not equal to the overall relative density. In this circumstances, σ_{fs} represents the strength of the strut (fibre network) in simple tension. De Ruvo *et al*. [23] approximated the in-plane strength of fibre networks by a power law function of the relative density which, using the nomenclature adopted here, gives an expression for σ_{fs}:

$$\sigma_{fs}/\sigma_f = k(1 - V_s)^n \quad (2)$$

where, σ_f is the tensile strength of the fibre itself, V_s is the volume fraction of porosity within the struts only, and k and n are constants. Values of n can vary from 1 to 4 depending on processing conditions. Equation 2 has the same form as Equation 1 and this indicates that the strength of the fibre network can be treated in a similar way to that of a cellular body. This can be further simplified by taking $k = 1/3$ and $n = 1$ reflecting the finding that the maximum tensile strength of a random two dimensional network is equal to one third of the strength of the individual component fibres [23, 24]. Thus

$$\frac{\sigma_{fs}}{\sigma_f} = \frac{1}{3}(1 - V_s). \quad (3)$$

The volume fractions V_p and V_s need to be determined separately and are related to the overall relative density, ρ^* by

$$V_s = 1 - \frac{\rho^*}{1 - V_p} \quad (4)$$

so that combining Equations 1, 3 and 4:

$$\sigma_{fc} = 1/15\sigma_f\rho^*(1 - V_p)^{1/2}. \quad (5)$$

Since the cells of the foam are large compared with the pores in the struts, they contribute little to sintering and the final pore volume fraction is comparable to the pore volume fraction in the as-foamed state. Taking the data from Table III, ρ^* is approximately 0.04. Taking manufacturer's data the as-received fibre has a tensile strength of 2 GPa but after heat treatment at 1200°C giving mainly alpha alumina, the strength is likely to be in the region of 500 MPa [14]. Equation 5 then predicts a compressive strength of 290 kPa, some 220 kPa higher than the measured value. Clearly the simplifications in Equation 3 need to be explored experimentally for the struts in which fibres tend to be uniaxially aligned; an arrangement that makes for a lower density of fibre contacts.

Equation 5 indicates that for a fibre foam with a given pore volume fraction V_p, the compressive strength of the foam σ_{fc} increases with the increase of the overall relative density ρ^* and with the increase of the relative density of the struts. Infiltration of the fibre foam by fine powder suspension slightly increases the relative density of the strut, and hence the compressive strength of the fibre foam, as shown in Table IV. However, Equation 5 does not take into account the effect of increasing the number density of contacts on the fibre bundles that make up the struts without significantly changing V_S. This was achieved by adding particles to the arrays. In fact, the number of junctions between the struts exerts a significant influence on the strength of the cellular body. In Fig. 6, a small number of junctions were formed between struts and the foam presented very low strength. Studies of dry-formed networks of fibres concluded [25] that the more well-bonded are the fibres are in the network, the larger must be the strain before the network yields. The incorporation of alumina powder in the foam increases the number density of bonds between the fibres, and the increase in strength is significant.

4. Conclusions

The use of a polyurethane foaming system for preparing a short staple ceramic fibre in cellular array has been demonstrated. The porous body produced in this way has a three dimensionally variable volume fraction of short fibres with interconnected open cells.

Attempts were made to increase the strength of the sintered preform by a) changing the sintering temperature, b) adding powder at the foaming stage, c) adding silicone oil at the foaming stage to leave a siliceous residue and d) infiltrating the sintered foam with an alumina powder suspension.

High temperature treatment, eg., sintering, caused phase transformation in the Saffil fibre from mainly delta-alumina to alpha-alumina and grain growth resulted in surface morphological changes. The use of silicone oil was not successful because of its low miscibility with the resin. By incorporating coarse alumina particles in the foam and by subsequent infiltration with fine alumina slurry, the compressive strength of the cellular body was significantly increased.

These cellular arrays of ceramic fibre have potential use in a range of applications, but the main aim of the present work was to prepare preforms for metal matrix composites which will produce a three dimensional bicontinuous microstructural topology.

Acknowledgement

The authors are grateful to EPSRC for the financial support of this work under Grant No. GR/L80553 and to Mr. Barrie Harvey of Vernaware, Bolton, UK for supplying the alumina fibre.

References

1. L. A. STROM, T. B. SWEETING, D. A. NORRIS and J. R. MORRIS, *Mater. Res. Soc. Symp. Proc.* **371** (1995) 321.
2. R. BREZNY and D. J. GREEN, *Acta. Metall. Mater.* **38** (1990) 2517.
3. J. SAGGIO-WOYANSKY, C. E. SCOTT and W. P. MINNEAR, *Amer. Ceram. Soc .Bull.* **71** (1992) 1674.
4. P. SEPULVEDA, *ibid.* **76** (1997) 61.
5. R. W. RICE, *Key Eng. Mater.* **115** (1996) 1.
6. Z. FAN, P. TAAKIROPOULOS and A. P. MIODOWNIK, *Mater. Sci. Tech.* **8** (1992) 922.
7. Z. FAN and A. P. MIODOWNIK, *Acta. Metall. Mater.* **41** (1993) 2403 and 2415.
8. Z. FAN, *Phil. Mag.* **73** (1996) 1663.
9. O. SIGMUND, *Mech. Mater.* **20** (1995) 352.
10. S. J. POWELL and J. R. G. EVANS, *Mater. Manuf. Proc.* **10** (1995) 757.
11. L. L. WOOD, P. MESSINA and K. C. FRISCH, U. S. Patent no. 3833386 (1974).
12. W. P. MINNEAR, in "Ceramic Transactions 26 : Foaming Science and Technology for Ceramics" (Amer. Ceram. Soc., Westerville, 1992) p. 149.
13. D. A. HIRSCHFELD, T. K. LI and D. M. LIU, *Key Eng. Mater.* **115** (1996) 65.
14. J. DINWOODIE, SAE Technical Paper Series, 870437, 1987.
15. H. X. PENG, Z. FAN, J. R. G. EVANS and J. J. C. BUSFIELD, *J. Euro. Ceram. Soc.* **20** (2000) 807.
16. J. D. BIRCHALL, J. A. A. BRADBURG and J. DINWOODIE, in "Strong Fibres" Vol. 1, in Handbook of Composites (North-Holland, 1988) p. 115.
17. P. A. BADKAR and J. E. BAILEY, *Mater. Sci. Res.* **6** (1973) 311.
18. J. V. MILEWSKI, *Ind. Eng. Chem. Prod. Res. Dev.* **17** (1978) 363.
19. S. BLACKBURN and H. BOHM, *J. Mater. Sci.* **29** (1994) 4157.
20. J. M. CHIOU and D. D. L. CHUNG, *ibid.* **28** (1993) 1435.
21. B. V. VELAMAKANNI, J. C. CHANG, F. F. LANGE and A. S. PEARSON, *Langmuir* **6** (1990) 1323.
22. L. J. GIBSON and M. F. ASHBY, "Cellular Solids: Structure and Properties," 2nd edn., Cambridge Solid State Science Series (Cambridge University Press, 1997) p. 209.
23. A. DE RUVO, C. FELLERS and P. KOLSETH, in "Paper Structure and Properties," edited by J. A. Bristow and P. Kolseth (Marcel Dekker Inc., New York, 1986) p. 267.
24. H. L. COX, *Br. J. Appl. Phys.* **3** (1952) 72.
25. C. ASKLING and L. WAGBERG, *J. Mater. Sci.* **33** (1998) 1517.

Received 7 October 1999
and accepted 25 May 2000